Article

Immunity

Poor Repair of Skeletal Muscle in Aging Mice Reflects a Defect in Local, Interleukin-33-Dependent Accumulation of Regulatory T Cells

Graphical Abstract

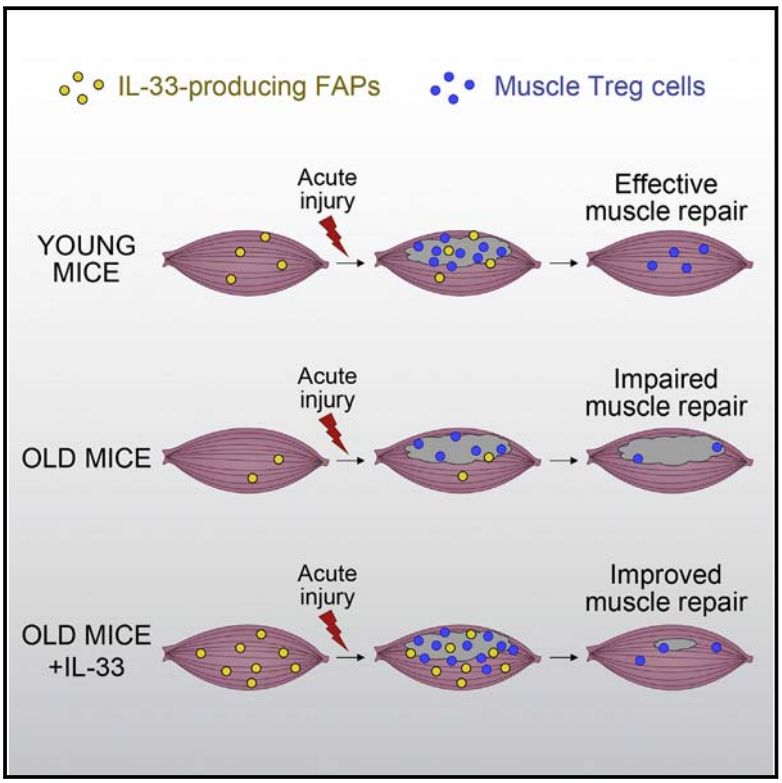

Authors

Wilson Kuswanto, Dalia Burzyn, Marisella Panduro, ..., Amy J. Wagers, Christophe Benoist, Diane Mathis

Correspondence

cbdm@hms.harvard.edu

In Brief

Aging is associated with decreased regenerative capacity of skeletal muscle. Mathis and colleagues find that reparative muscle Treg cells do not accumulate in acutely injured muscle of old mice. IL-33 regulates muscle Treg cell homeostasis, and its administration improves muscle Treg cell accumulation and muscle regeneration in old mice.

Highlights

- Muscle regulatory T (Treg) cells, which aid muscle repair, are reduced in aged mice
- IL-33 regulates muscle Treg cell dynamics; its injection into old mice improves repair
- Fibro/adipogenic progenitors (FAPs) are the major IL-33-producing cells in muscle
- IL-33^{+} FAPs are often closely apposed to nerve structures in skeletal muscle

Accession Numbers

GSE76722
GSE76733
GSE76695
GSE76697

Kuswanto et al., 2016, Immunity *44*, 355–367
February 16, 2016
http://dx.doi.org/10.1016/j.immuni.2016.01.009

CellPress

Immunity
Article

Poor Repair of Skeletal Muscle in Aging Mice Reflects a Defect in Local, Interleukin-33-Dependent Accumulation of Regulatory T Cells

Wilson Kuswanto,[1,7] Dalia Burzyn,[1,7,8] Marisella Panduro,[1] Kathy K. Wang,[1] Young Charles Jang,[2,3,9] Amy J. Wagers,[2,3,4,5] Christophe Benoist,[1,6] and Diane Mathis[1,6,*]
[1]Microbiology and Immunobiology, Harvard Medical School, Boston, MA 02115, USA
[2]Stem Cell and Regenerative Biology, Harvard University, Cambridge, MA 02138, USA
[3]Howard Hughes Medical Institute, Chevy Chase, MD 20815, USA
[4]Joslin Diabetes Center, Boston, MA 02215, USA
[5]Paul F Glenn Center for the Biology of Aging, Harvard Medical School, Boston, MA 02115, USA
[6]Evergrande Center for Immunologic Diseases, Harvard Medical School and Brigham and Women's Hospital, Boston, MA 02115, USA
[7]Co-first author
[8]Present address: Jounce Therapeutics, Inc., Cambridge, MA 02138, USA
[9]Present address: Georgia Institute of Technology, Atlanta, GA 30332, USA
*Correspondence: cbdm@hms.harvard.edu
http://dx.doi.org/10.1016/j.immuni.2016.01.009

SUMMARY

Normal repair of skeletal muscle requires local expansion of a special population of Foxp3$^+$CD4$^+$ regulatory T (Treg) cells. Such cells failed to accumulate in acutely injured muscle of old mice, known to undergo ineffectual repair. This defect reflected reduced recruitment of Treg cells to injured muscle, as well as less proliferation and retention therein. Interleukin-33 (IL-33) regulated muscle Treg cell homeostasis in young mice, and its administration to old mice ameliorated their deficits in Treg cell accumulation and muscle regeneration. The major IL-33-expressing cells in skeletal muscle displayed a constellation of markers diagnostic of fibro/adipogenic progenitor cells and were often associated with neural structures, including nerve fibers, nerve bundles, and muscle spindles, which are stretch-sensitive mechanoreceptors important for proprioception. IL-33$^+$ cells were more frequent after muscle injury and were reduced in old mice. IL-33 is well situated to relay signals between the nervous and immune systems within the muscle context.

INTRODUCTION

Foxp3$^+$CD4$^+$ regulatory T (Treg) cells play a key role in immune-system homeostasis. Classically, they have been associated with various types of immune responses, but more recently, they were found to operate in diverse non-immunological contexts as well. For example, visceral-adipose-tissue (VAT) Treg cells regulate local and systemic inflammation and metabolism (Feuerer et al., 2009), and a distinct population of Treg cells in skeletal muscle potentiates regeneration in acute and chronic injury models (Burzyn et al., 2013). At both of these sites, Treg cells can exert a direct influence on local parenchymal cells or their progenitors, in addition to regulating macrophage activities.

Skeletal muscle is a highly specialized tissue composed largely of post-mitotic, multinucleate cells (myofibers) that rarely turn over in the absence of damage. Upon injury, muscle mounts a robust regenerative response that supports repair or replacement of almost all of the neighboring myofibers. Muscle regeneration is dependent on a pool of quiescent, committed, self-renewable precursors, called satellite cells, found beneath the basal lamina in juxtaposition to muscle fibers (Jang et al., 2011). Injury induces satellite cells to become activated, proliferate, differentiate, and either form new myofibers or fuse to existing ones. Leukocytes such as neutrophils, eosinophils, monocytes, and macrophages are critical to the regenerative response, arriving within hours of injury; CD4$^+$ and CD8$^+$ T cells join in over time and are generally thought to impede tissue repair (Tidball and Villalta, 2010; Heredia et al., 2013). In contrast, Treg cells enhance repair, accumulating in both acute and chronically injured muscle to constitute 40%–50% of CD4$^+$ T cells (Burzyn et al., 2013; Villalta et al., 2014), well above the typical circulating frequency of 10%–15%. The increase in Treg cell representation correlates with a switch in myeloid-lineage populations from a pro- to an anti-inflammatory phenotype, and punctual depletion of Treg cells inhibits this phenotypic switch (Burzyn et al., 2013). Muscle Treg cells display a distinct, clonally expanded, T cell receptor (TCR) repertoire that shows signs of antigenic selection. The muscle Treg cell transcriptome, although enriched for signature transcripts, differs substantially from those of Treg cells found in lymphoid tissues.

Aging of skeletal muscle, like that of most mammalian tissues, is associated with a steady decline in both function and regenerative capacity (Jang et al., 2011). The defect in regeneration is due at least in part to an age-associated decrease in satellite cell frequency and function. The molecular mechanisms underlying reduction of the satellite pool are the focus of ongoing investigation, with studies on heterochronic parabiotic mice

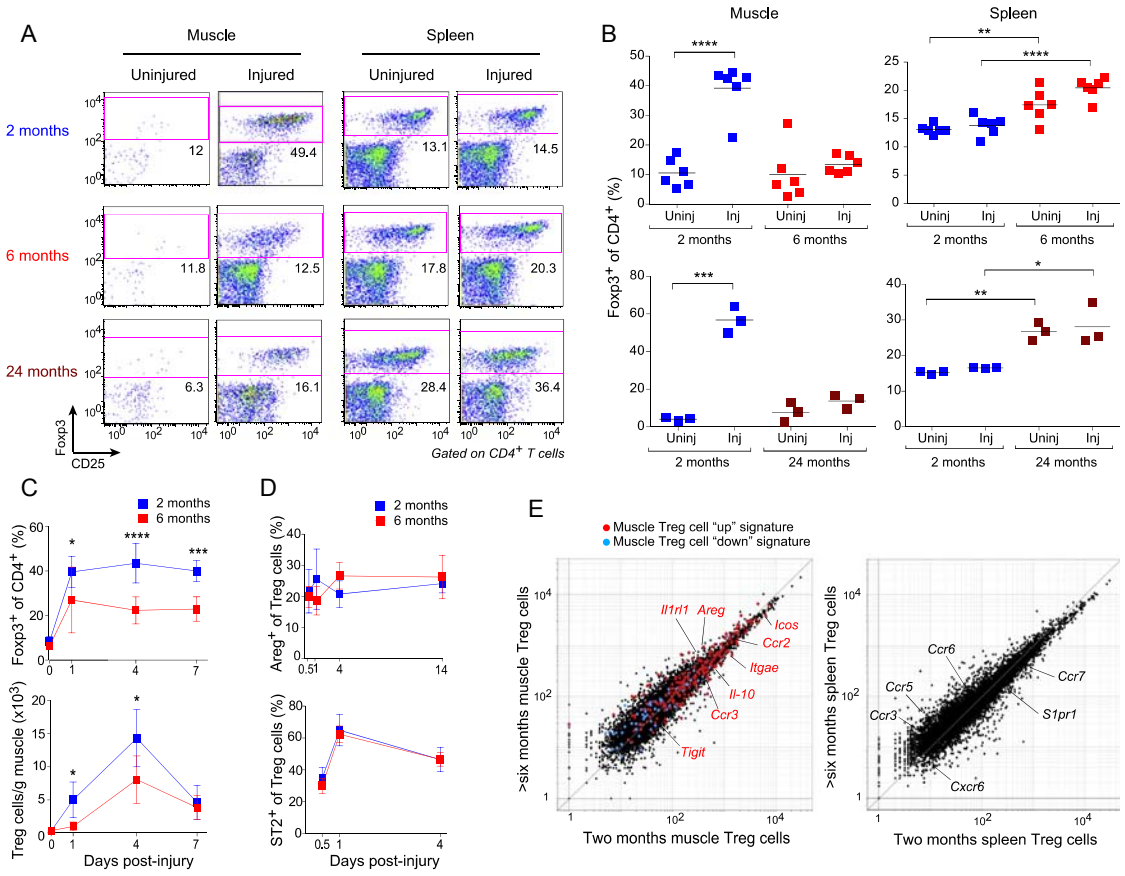

Figure 1. Diminished Treg Cell Accumulation in Skeletal Muscle of Aged Mice

Different-aged B6 mice were i.m.-injected with CTX into the hindlimb muscles.

(A) Cytofluorometric dot plots of lymphocytes taken 6 days after injury. Representative of n = 3–6 mice. Numbers depict the fraction of $CD4^+$ T cells within the designated gate.

(B) Summary data for the experiments depicted in (A).

(C) Summary data on Treg cell fraction (top) and number (bottom) various days after injury. n = 4–9.

(D) Summary data on muscle Treg cell diagnostic marker expression over time. n = 4 mice.

(E) RNA-seq analysis. Normalized expression values for muscle (left) and splenic (right) Treg cells isolated 4 days after CTX injury. Muscle Treg cell "up" (red) and "down" (blue) signature transcripts (Burzyn et al., 2013) are overlain in the left panel, with some key muscle Treg cell "up" genes highlighted. Some differentially expressed genes encoding trafficking or related molecules are highlighted on the spleen plot in the right panel. Averaged from two experiments.

For all relevant panels: mean ± SD. *p ≤ 0.05; **p ≤ 0.01; ***p ≤ 0.001; ****p ≤ 0.0001 from the unpaired t test corrected for multiple experiments. Post-test comparisons of ranked p values (generated from Fisher's least significant difference test) using the Holm-Sidlac method. Significance level set at 5%. All other p values were not significant. See also Figure S1.

suggesting an important contribution of circulating factors and/or migratory immune-system cells (Conboy et al., 2005; Brack et al., 2007; Sinha et al., 2014). Treg cell representation within lymphoid tissues has repeatedly been shown to increase with age (Nikolich-Žugich, 2014), yet little is known about concomitant effects on their trafficking to and function within nonlymphoid tissues in response to various challenges.

Here we address whether numerical or phenotypic alterations in local Treg cells subtend the poor muscle regeneration of old mice. We report a severe age-dependent decline in Treg cell accumulation in injured skeletal muscle and go on to explore the population dynamics underlying this reduction. We uncover the importance of the interleukin (IL)-33:ST2 axis in muscle Treg cell accumulation and function, exploit this axis to enhance muscle repair in old mice, and uncover an unexpected physical association between IL-33-producing stromal cells and nerve cells in muscle.

RESULTS

Treg Cell Accumulation Is Diminished in Acutely Injured Skeletal Muscle of Aged Mice

Treg cells represent about 10% of the $CD4^+$ T cell compartment in uninjured skeletal muscle of C57BL/6 (B6) mice, a frequency that does not change with age (Figures 1A and 1B). In young mice (≤2 months of age), acute muscle injury, generated either by injection of cardiotoxin (CTX) or via milder cryoinjury, results in the accumulation of a distinct population of Treg cells within days (Figures 1A and 1B; Burzyn et al., 2013). However, such an increase was not observed in old mice (≥24 months of age),

a difference that was apparent already at 6 months (Figures 1A and 1B). In contrast, irrespective of muscle injury, the two older groups showed an elevated frequency of splenic Treg cells, as previously reported (Nikolich-Žugich, 2014). The reduced accumulation of Treg cells in muscle of aged mice was observed throughout the time course of recovery from CTX-induced injury (Figure 1C).

The Treg cells that were found in the injured muscle of older mice were bona fide "muscle Treg cells" as shown by the fact that they displayed typical amounts of diagnostic cell-surface markers, such as ST2 (the IL-33 receptor) and amphiregulin (Areg) (Figure 1D; Burzyn et al., 2013). They also expressed the characteristic muscle Treg cell "up" and "down" signatures (Burzyn et al., 2013), according to RNA-seq analysis of cells harvested 4 days after injury (Figure 1E).

Given their reported roles in skeletal muscle regeneration (Arnold et al., 2007) and their sensitivity to Treg cell numbers and activities (Burzyn et al., 2013), we also compared the myeloid-lineage populations that arose after CTX injury of young and aged mice. There was a significant decrease in representation of the major histocompatibility complex class II (MHCII)-negative compartment of monocytes plus macrophages in aged mice (Figures S1A and S1B), a change parallel to that provoked by punctual ablation of Treg cells in young mice (M.P., C.B., and D.M., unpublished results).

Reduced Treg Cell Accumulation in Injured Muscle of Aged Mice Reflects Defects in their Recruitment, Proliferation, and Retention

Next we sought to identify the feature(s) of muscle Treg cell population dynamics that were compromised in older mice. As a prelude, we determined whether muscle Treg cell accumulation in young mice was dependent on recruitment from the pool of circulating T cells. 2-month-old mice were treated with the S1P1 receptor agonist, FTY720, at the same time as CTX injury, and muscle infiltrates were analyzed by flow cytometry over a 7-day time course. Agonism of the S1P1 receptor provokes its downregulation, thereby trapping T and B cells within lymphoid tissues and clearing them from the circulation (Kunkel et al., 2013). Although FTY720 treatment had no significant effect on the overall size of the cellular infiltrate in injured muscle, it profoundly reduced the accumulation of Treg cells (Figure 2A). Thus, the accrual of muscle Treg cells in response to injury seemed to depend on recruitment from the circulating T cell pool.

These results raised the possibility that the reduced accumulation of Treg cells in injured muscle of older mice reflected a defect in their recruitment to the muscle, their proliferation, and/or their retention therein. Because FTY720 can affect processes other than egress from lymphoid tissues, we turned to the Kaede transgenic (Tg) mouse system (Tomura et al., 2008) both to confirm the conclusions from the FTY720 experiments and to evaluate the three possible mechanisms. Kaede/B6 mice ubiquitously express a photoconvertible fluorescent reporter (Kaede) under the control of *Actb* transcriptional control elements. Upon exposure to violet light, reporter fluorescence irreversibly converts from green to red, innocuously and stably for at least 2 weeks. 1 day after CTX-induced muscle injury, we non-invasively photoconverted cells in the cervical lymph nodes (CLNs) of 2-month-old or >6-month-old mice by exposure to violet light; Kaede-red$^+$ cells were then tracked from the CLNs (representing the general circulation) to the axillary LNs (ALNs, general circulation), the inguinal LNs (ILNs, muscle-draining), and the muscle (Figure 2B). At 24 hr after photoconversion, about half of the Kaede-red$^+$ Treg cells had emigrated from the CLNs in young mice, whereas significantly fewer (only a quarter) had done so in aged individuals (Figures 2C and 2D). A similar age-dependent difference in emigration from the CLNs was observed for Kaede-red$^+$ conventional CD4$^+$ T (Tconv) cells (Figure 2D). Accordingly, a lower frequency of photoconverted cells was found in the CD4$^+$ T cell compartments of injured muscles, the draining ILNs, and the non-draining ALNs of aged mice (Figure S2A). When the muscle and ILN fractions were normalized to the ALN values in order to correct for general circulation patterns, it became clear that the major migration-related difference between young and aged mice concerned migration of Treg cells to the injured muscle (Figure 2E): vigorous in young mice, actually double that of the general circulation (i.e., the migation ratio was □2), but barely detectable in their aged counterparts. This difference was not found for Tconv cells.

To uncover any age-related effects on Treg cell proliferation, we injected mice with 5-ethynyl-2^0-deoxyuridine (EdU) at the time of CTX-induced injury and quantified its incorporation by CD4$^+$ T cell subsets at relevant sites. Proliferation of Treg cells from injured muscle, but not the spleen, of aged mice was clearly reduced vis-à-vis young individuals (Figures 2F and S2B). No such difference was seen for Tconv cells.

For evaluation of the age dependence of Treg cell retention in injured muscle, we again turned to the Kaede Tg system, but this time photoconverted the injured tibialis anterior (TA) muscle (Figure 2G). The decay curve of the photoconverted Treg cell population in injured muscle revealed an increased turnover in aged relative to young mice (Figure 2H). Enhanced turnover of muscle Treg cells in aged mice was due, at least in part, to increased migration from the injured muscle to the ILNs and ALNs (Figure 2I). (Note that the high values in ILNs at later times, a few even R 100%, probably reflect proliferation.)

The IL-33:ST2 Axis Impacts Muscle Treg Cell Accumulation and Regenerative Activities

An obvious question was what factor(s) might promote the accumulation of Treg cells in injured skeletal muscle of young mice. Our attention was rapidly drawn to IL-33 because *Il1rl1*, which encodes this cytokine's receptor, ST2, was one of the loci most strongly upregulated in muscle versus lymphoid-tissue Treg cells (Figure 3A) and because recent work has linked IL-33 to the control of Treg cell homeostasis in parenchymal tissues (Schiering et al., 2014; Vasanthakumar et al., 2015; Kolodin et al., 2015). ST2 protein was also upregulated at the surface of muscle Treg cells, measured as either the fraction of ST2$^+$ cells or the ST2 MFI (Figure 3B). An elevated fraction of ST2$^+$ Treg cells was evident in muscle as early as 12 hr after injury, peaked on day 2, then dipped from day 4 onward, but to a value (□30%) still substantially higher than that of lymphoid-tissue Treg cells (<5%) (Figure 3C). Such frequent expression of ST2 was not a general feature of cells infiltrating injured skeletal muscle; it was not observed for either neutrophils, monocytes, or macrophages (Figure 3C).

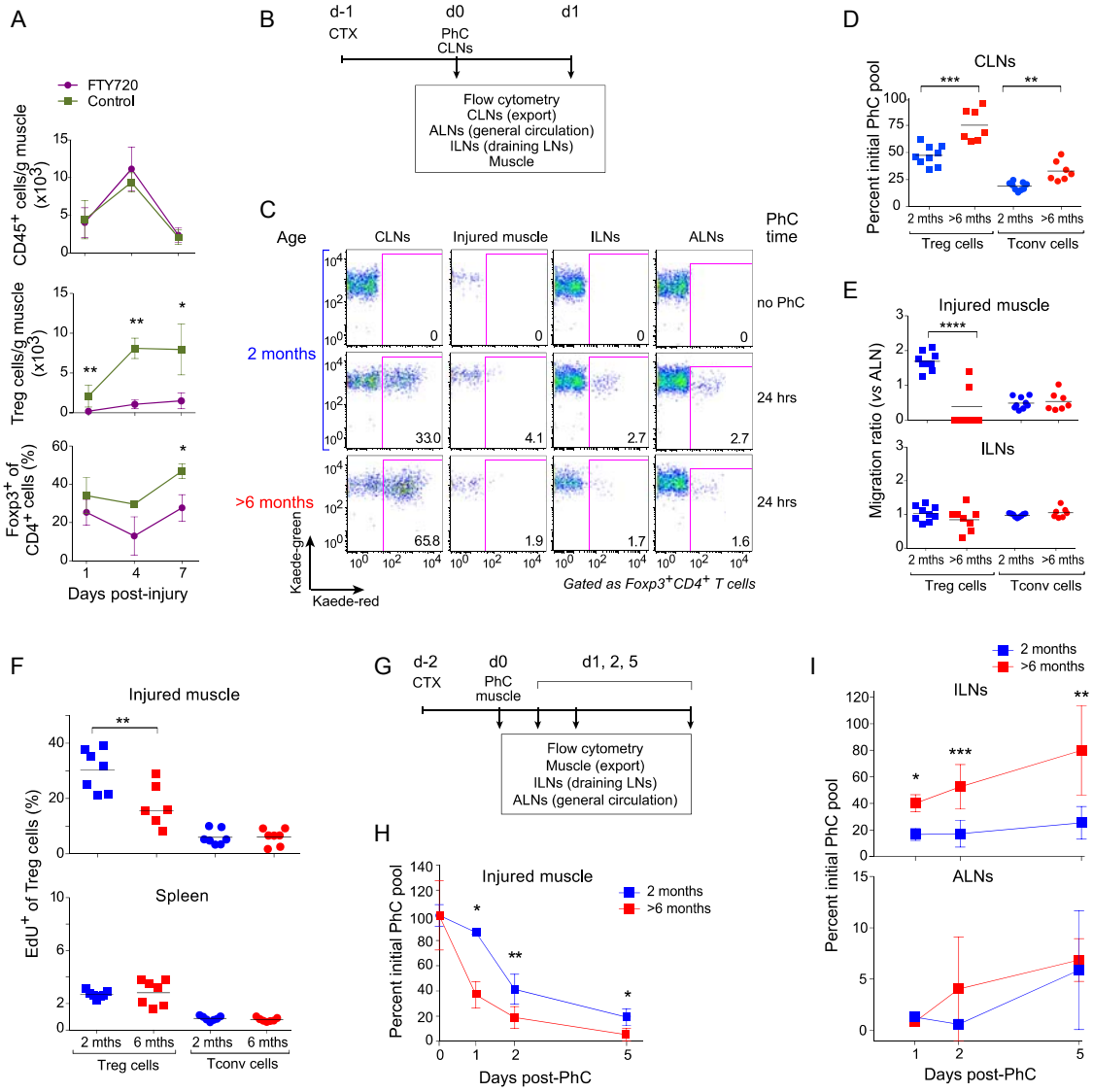

Figure 2. Defects in Treg Cell Recruitment, Proliferation, and Retention in Muscle of Aged Mice

(A) Muscle Treg cell dependence on the circulating pool. 2-month-old mice were treated with FTY720 or PBS a day prior to CTX-induced injury and daily thereafter, and muscle lymphocytes were analyzed cytofluorometrically various days later. n = 3–8 mice.

(B–E) Treg cell migration from the CLNs to the muscle.

(B) Schematic diagram of the protocol. 2-month-old or >6-month-old Kaede/B6 Tg mice were injected with CTX, and 24 hr later, the CLNs (cervical LNs) were exposed to violet light non-invasively. Lymphocytes from the indicated tissues were examined cytofluorometrically for Kaede-red$^+$ photoconverted (PhC) cells, either immediately or 24 hr later (abbreviations are as follows: ALNs, axial LNs; ILNs, inguinal LNs).

(C) Dot plot representative of n = 7–9 mice from three experiments.

(D) Exodus from the PhC CLN pool. Normalized to the day 0 PhC population.

(E) Immigration to various tissues. The "migration ratio" is the fraction of Kaede-red$^+$ cells in a designated organ normalized to the fraction in the non-draining LN, which provides a measure of the systemic circulation. Raw fractional data appear in Figure S2A.

(F) Muscle Treg cell proliferation. EdU was co-injected at the time of CTX injury, and LNs from the indicated tissues were examined cytofluorometrically a day later. n = 7 mice from two experiments. Representative dot plots can be found in Figure S2B.

(G–I) Treg cell migration out of the muscle.

(G) Schematic diagram of the protocol. As in (B)–(D), except that the tibialis anterior muscle was exposed to violet light 2 days after CTX injection, and tissues were examined 1–5 days later.

(H) Emigration of the initial PhC pool from the muscle. n = 2–9 mice from three experiments. Normalized to the day 0 PhC population.

(I) Immigration of the initial PhC pool to draining and non-draining LNs. Normalized to the day 0 PhC value. Values R 100% probably reflect proliferation.

Statistics for this figure as per Figure 1. See also Figure S2.

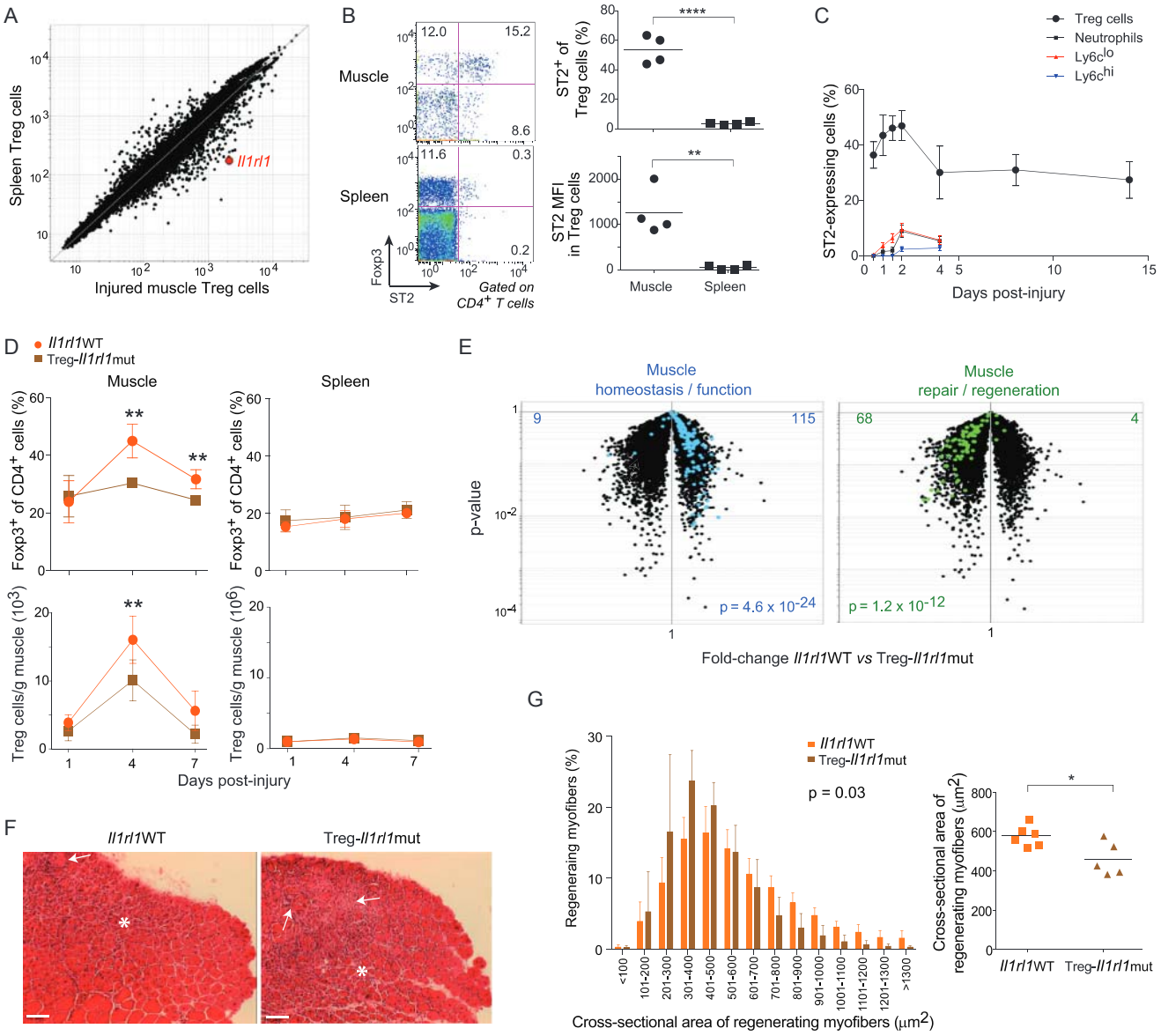

Figure 3. Involvement of the IL-33:ST2 Axis in Muscle Treg Cell Accumulation and Regenerative Activities

(A) Microarray analysis. Normalized expression values for Treg cells from 2-month-old mice isolated 14 days after CTX injury. Data from Burzyn et al. (2013).

(B) Cytofluorometric analysis. Hindlimb muscles from 2-month-old mice were prepared a day after CTX injury. Left, dot plots representative of n = 4 mice from two experiments. Numbers depict fraction of $CD4^+$ T cells. Right, summary data for fraction of $ST2^+$ Treg cells (top) and Treg cell ST2 mean fluorescence intensity (MFI) (bottom).

(C) Summary data for ST2 fraction within various leukocyte populations at various times after CTX injury of 2-month-old mice. n = 3–8 mice from two experiments.

(D) Impact of Treg-cell-expressed ST2 on Treg cell accumulation. 2-month-old mice with a Treg-cell-specific ablation of ST2 expression (*Il1rl1*mut) or their homozygous wild-type littermates (*Il1rl1*WT) were injected with CTX, and Treg cells were examined cytofluorometrically various times later. Top, fractional representation; bottom, numbers. Summary data for n = 4–7 mice from two experiments.

(E–G) Impact of Treg-cell-expressed ST2 on muscle repair 4 days after cryoinjury.

(E) Expression of diagnostic transcript signatures. Microarray analysis was performed on RNA isolated from whole muscle of 2-month-old mice taken 8 days after cryoinjury. Overlain are signatures developed and validated in Burzyn et al. (2013); transcript identities are listed in Table S1 for convenience.

(F) Histologic appearance. Representative H&E stains of tibialis anterior muscle from 2-month-old mice taken 8 days after cryoinjury (representative of two experiments). Arrows highlight necrotic areas, and asterisks indicate cellular infiltration. Original magnification = 1003 . Scale bars represent 100 mm.

(G) Quantification of regenerating fibers. For the mice illustrated in (F), the cross-sectional area of regenerating myofibers is represented as a frequency distribution of myofiber size (left) or as the mean area (right). n = 5–6 mice from two experiments.

p values in this figure as per Figure 1, except that those of (E) come from the chi-square test and from the left graph of (G) from the t test of weighted sum. See also Table S1.

To test the possible involvement of the IL-33:ST2 axis in muscle Treg cell accumulation and function, we generated mice lacking ST2 specifically on Treg cells (Treg-*Il1rl1*mut), always comparing their performance with that of wild-type (WT) littermates (*Il1rl1*WT). Cytofluorimetrically, the representation of muscle Treg cells in 2-month-old mutant and WT mice was similar 1 day after CTX-induced injury; however, ST2-denuded Treg cells showed impaired accumulation over time (Figure 3D). In contrast, there was no significant difference in the splenic Treg cell populations of mutant and WT mice (Figure 3D). Flow cytometry confirmed that Treg cells in the mutant mice were all devoid of ST2 (data not shown).

Several assays were employed to assess the importance of Treg cell expression of ST2 for muscle regeneration. In order to facilitate cross-mouse quantification and comparison, we cryoinjured TA muscles, a method that provokes milder, more uniform injury and permits better visualization than CTX-induced injury does. There was also a significant reduction in the accumulation of Treg cells in muscle of Treg-*Il1rl1*mut mice 4 days after cryoinjury, in particular those with a bona fide muscle Treg cell phenotype signaled by Klrg1 expression (Burzyn et al., 2013; data not show). Regeneration was initially evaluated via whole-tissue transcriptomics, making use of signatures developed and validated in our previously published kinetic analysis of skeletal muscle regeneration (Table S1; Burzyn et al., 2013). Expression of a set of "muscle homeostasis/function" genes is routinely high at steady-state, decreases for several days after acute injury (d4), and returns to steady-state values once regeneration has been completed (d8). Examples include genes whose products are implicated in metabolism (*Pfkfb1*, *Adh1*, *Fbp2*, and *Vldlr*) or muscle differentiation and function (*Mstn* and *Mb*). This signature was strongly under-represented in mutant, vis-à-vis WT, muscle Treg cells 8 days after injury (Figure 3E, left). In contrast, expression of a set of "muscle repair/regeneration" genes is routinely very low at steady-state, increases over the first days after injury (4d), and eventually, and obligatorily, returns to the low baseline values (8d). The products of these genes promote efficient tissue repair, e.g., *Myog* (which encodes a muscle transcription factor), *Mmp2*, and *Adam8* (encoding proteins involved in construction of the extracellular matrix). This signature was substantially over-represented in the muscle Treg cells of mutant mice 8 days after injury (Figure 3E, right). These transcriptional aberrations were accompanied by histological abnormalities, e.g., less effective clearing of the muscle infiltrate in the absence of ST2 (Figure 3F). Furthermore, the distribution and mean cross-sectional area of regenerating (centrally nucleated) myofibers was significantly decreased in mice lacking ST2 specifically on Treg cells (Figure 3G), indicating delayed or impaired recovery from injury. Thus, the IL-33:ST2 axis plays a clear role in the accumulation and pro-regenerative activities of the Treg cells associated with acutely injured muscle of young mice.

Muscle IL-33 Expression Spikes Shortly after Acute Injury, Reflecting Synthesis by Nerve-Associated Cells Resembling Fibro/Adipogenic Progenitors

IL-33 is a member of the IL-1 family of cytokines (Cayrol and Girard, 2014). It resides constitutively in the nucleus, primarily of non-hematopoietic cells, including epithelial cells, endothelial cells, and fibroblasts. In response to stimuli such as infectious agents, allergens, or mechanical perturbation, IL-33 is released from the cell by a mechanism that remains obscure, but entails, at least in part, passive release from necrotic or stressed cells. Demonstration of a role for IL-33 in injury-induced expansion of the muscle Treg cell population and in optimal muscle regeneration after injury raised the issue of this cytokine's synthesis in skeletal muscle. How does IL-33 expression change in response to acute injury? What cells produce it? How does IL-33 expression evolve with aging?

Both *Il33* transcript quantification by PCR titering (Figure 4A) and IL-33 protein estimation by immunoblotting (Figure 4B) revealed a spike of expression 6–12 hr after acute muscle injury. As a first step toward pinpointing the cells producing IL-33, we sorted the $CD45^+$ and $CD45^-$ fractions of the myofiber-associated (MFA) and interstitial muscle compartments 12 hr after injury and quantified transcripts via PCR analysis. For both compartments, the major IL-33 expressers were $CD45^-$ cells (Figure 4C). This finding was confirmed by both immunohistology (Figure S3B) and flow cytometry (see below), which also failed to evidence many IL-33^+ endothelial ($CD31^+$) cells (Figure S3C and see below).

Given their fibroblastic nature and documented role in skeletal muscle regeneration (Joe et al., 2010; Uezumi et al., 2010; Murphy et al., 2011), fibro/adipogenic progenitor (FAP) cells emerged as a promising candidate. These cells are characterized by surface display of Sca1 and the alpha chain of the receptor for platelet-derived growth factor (PDGFRa) in the absence of CD45, CD31, and other hematopoietic lineage markers (lin^-). Indeed, cytofluorometric studies revealed that the major IL-33^+ cell population in both uninjured and injured muscle of young mice displayed this constellation of markers, in addition to expressing podoplanin (Gp38, PDPN) (Figures 4D and 4E). Injury increased the representation of IL-33^+ FAPs (Figure 4E).

Immunohistological analyses confirmed the overlap between IL-33 synthesis and PDGFRa display, as well as providing information on this cytokine's cellular and intracellular geography in muscle. Low-magnification scanning revealed IL-33-expressing cells to be most abundant in regions immediately surrounding muscle fibers (Figure S3A). Many of them (~20%), were intimately associated with nerve structures. IL-33 was readily detected within $PDGFRa^+$ cells of the perineurium ($Glut1^+$) encasing the myelin sheath ($S100^+$) of nerve fibers (Figure 5A), within nerve bundles (Figure 5B), and within cells parenthesizing muscle spindles (Figure 5C). Muscle spindles are collections of nerves and specialized muscle fibers (intra- and extra-fusal) surrounded by a fibrous capsule and are critical in stretch-sensitive mechanoreception and thereby proprioception (Maier, 1997). Only in cells associated with muscle spindles could we detect IL-33 in the cytoplasm (Figure 5C). Within 12 hr of CTX-induced injury, there was a global increase in IL-33^+ cells, not obviously confined to a particular region or cell type—both "by eye" and according to the fraction of $DAPI^+$ structures (nuclei) co-expressing IL-33 (Figure 5D).

We were also able to detect IL-33-expressing cells in biopsies of uninjured gluteus maximus from healthy humans. Again, many of them could be found in association with nerve structures, notably nerve fibers meandering through the muscle (Figure 5E, left). In contrast to mice, humans also expressed IL-33 in cells associated with vascular structures (Figure 5E, right).

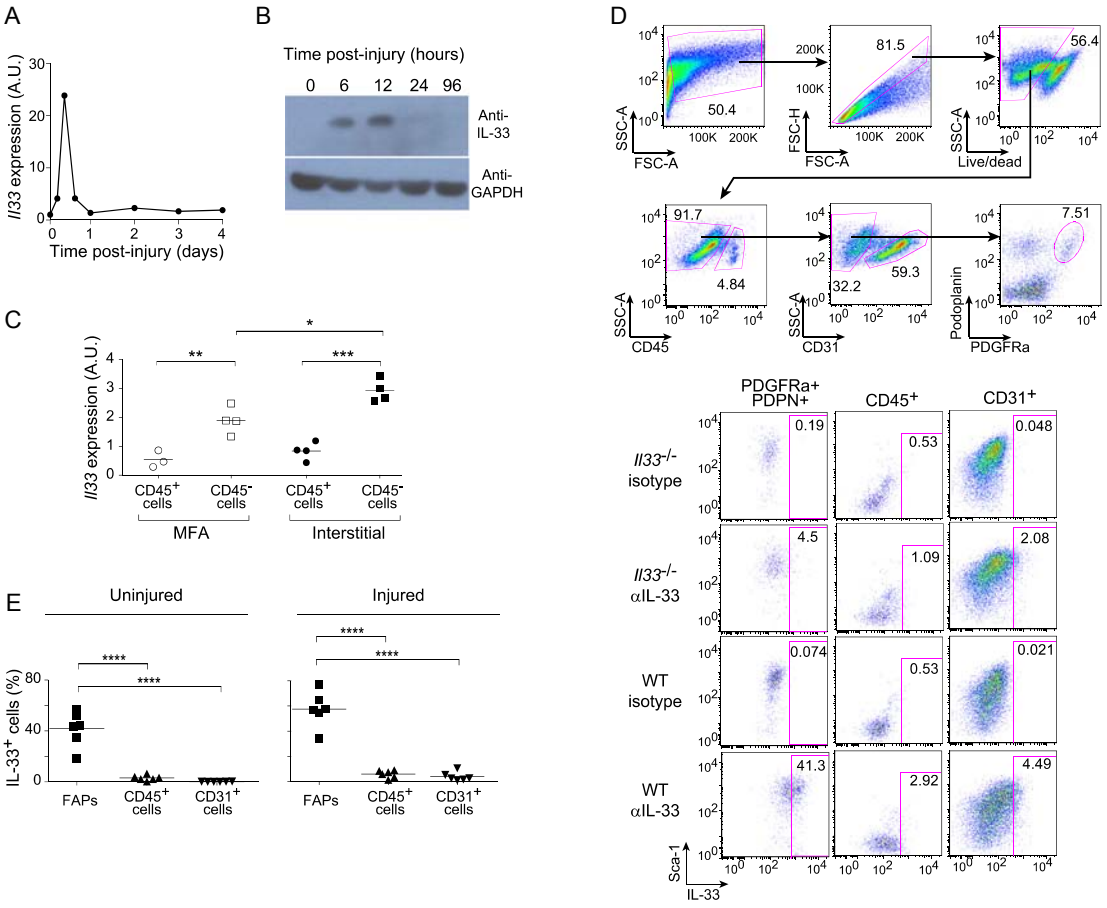

Figure 4. Quantification of IL-33 Expression and Identification of IL-33 Expressers as Cells Resembling FAPs

(A and B) An early spike of IL-33 expression. 2-month-old mice were injected with CTX, and various times later, *Il33* transcripts in tibialis anterior muscle were quantified by PCR (A) or IL-33 protein was estimated by immunoblotting (B). Plotted in (A) is the fold-change in expression value relative to that of uninjured muscle. For PCR, n = 2 mice. For immunoblotting, n = 1 (24 and 96 hr) to 3 (uninjured, 6 and 12 hr) mice.

(C) Localization of IL-33 expression within muscle. *Il33* transcripts in the myofiber associated (MFA) and interstitial muscle compartments were quantified by PCR 12 hr after CTX injury of 2-month-old mice. Data are represented as fold-change relative to the corresponding population from uninjured muscle. n = 3–4 mice from two experiments.

(D) Gating strategy to localize IL-33 expression by flow cytometry. Single-cell suspensions were prepared from uninjured hindlimb muscles of *Il33*$^{\square/\square}$ mice and WT controls and were analyzed by flow cytometry for the indicated markers. Top row of plots: gating strategy to delineate hematopoetic cells (CD45$^+$), endothelial cells (CD31$^+$), and FAPs (CD45$^{\square}$CD31$^{\square}$PDGFRa$^+$PDPN$^+$). Lower set of plots: typical staining for IL-33, including isotype and IL-33-deficient negative controls. Numbers indicate the fraction of cells in the gated population.

(E) Summary data on uninjured (top) and 12 hr after CTX-injured (bottom) muscle. n = 6 mice from two experiments.

Statistical analysis of this figure's data as per Figure 1. See also Figure S3.

Lastly, we compared IL-33 expression in injured muscle of young and aged mice, employing a variety of assays. *Il33* transcript values 6 hr after CTX-induced injury were significantly higher in young individuals (Figure 6A). This trend held, although less strikingly, at 12 hr. We also observed fewer IL-33$^+$ FAPs when quantified cytofluorometrically (Figure 6B). Inexplicably, we did not see a parallel difference in IL-33 protein expression by immunoblotting (data not shown).

Exogenous Addition of IL-33 Restores the Treg Cell Population in Injured Muscle of Aged Mice, Enhancing Regeneration

Injection of IL-33 can augment the fraction and number of Treg cells in parenchymal tissues within just a few days (Schiering et al., 2014; Vasanthakumar et al., 2015; Kolodin et al., 2015), and values can remain elevated for at least a month afterward (Kolodin et al., 2015). To determine whether IL-33 could boost the Treg cell population in injured muscle, we injected different-aged mice with recombinant IL-33 or just vehicle (phosphate-buffered saline [PBS]) on the day of injury and analyzed them by flow cytometry 6 days later. IL-33 did indeed expand the muscle Treg cell population; in IL-33-treated 6-month-old mice, the numbers attained were even greater than those typical of IL-33-untreated 2-month-old individuals (Figure 7A, left). In contrast, there was no significant increase in the size of the splenic Treg cell populations under these conditions (Figure 7A, right). Neither was there an augmentation of the muscle or spleen Tconv cell compartments (Figure S4A).

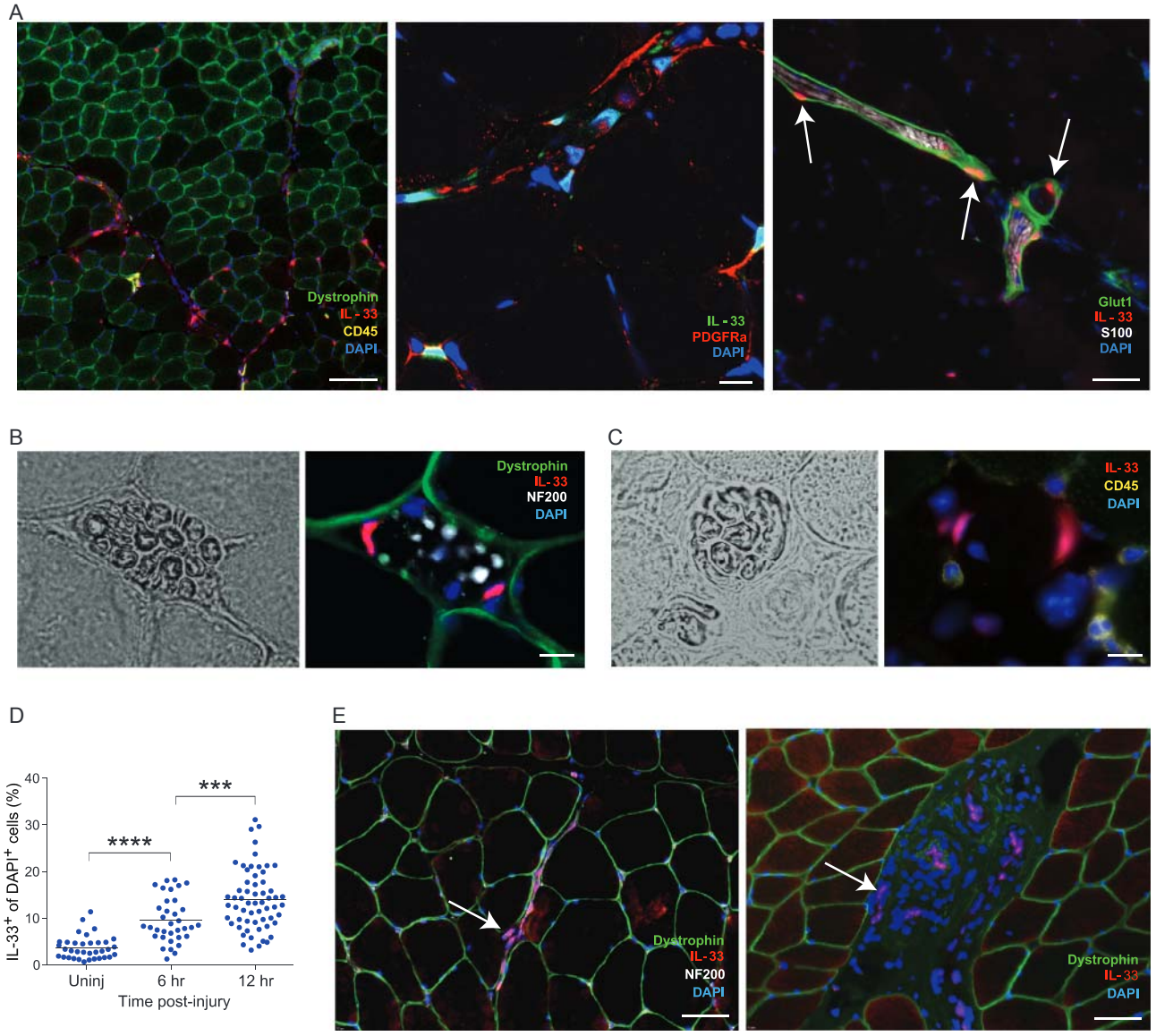

Figure 5. Immunohistologic Localization of IL-33-Expressing Cells in Mice and Humans

(A–C) Co-localization of IL-33$^+$ cells within nerve structures: in PDGFRa$^+$ cells of the perineurium (Glut1$^+$) encasing myelin sheaths (S100$^+$) of nerve fibers (A), in nerve bundles (B), or in muscle spindles (C). Immunofluorescence microscopy of muscle sections 6 hr after CTX injury. Left panels in (B) and (C) are brightfield views. Original magnifications are as follows: (A, right), (B), and (C) = 200× ; (A, left) = 100× ; (A, center) = 600× . Scale bars represent 100 mm (A, left), 10 mm (A, middle, B, C), and 50 mm (A, right).

(D) Increase in IL-33$^+$ cells upon muscle injury. The fraction of IL-33$^+$ nuclei (DAPI$^+$ structures) was measured automatically as described in the Experimental Procedures. p < 0.0001 by an unpaired t test. Each dot represents a single field of view. Data from 4–10 fields from 2–3 individual mice.

(E) IL-33-expressing cells in human muscle. Uninjured gluteus maximus from healthy individuals (representative of three examined). Left, IL-33$^+$ cells surrounding nerve fibers; right, vascular IL-33$^+$ cells. Original magnification is 200× . For all panels, arrows point to IL-33$^+$ cells. Scale bar represents 50 mm.

As a first step in addressing the mechanisms involved, we determined whether IL-33 boosted the recruitment of Treg cells from the circulation via the Kaede Tg mouse experiment depicted in Figure S4B. Young mice were treated with IL-33 or vehicle alone at the time of injury; a day later, the CLNs were photoconverted; and again a day later, total, ST2$^+$, and Kaede-red$^+$ Treg cells were quantified from the muscle and control ALNs. Although IL-33 increased the representation of Treg cells in the CD4$^+$ T cell compartment (Figure S4C, left) and the fraction of Treg cells expressing ST2 (Figure S4C, right), as anticipated, it did not enhance the recruitment of circulating Treg cells to the muscle (Figures S4D and S4E). IL-33 did, however, have a strong impact on Treg cell proliferation, as evidenced by the experiment schematized in Figure S5A. Two and a half days after CTX-induced muscle injury, old mice were injected with EdU; and 12 hr later, total, ST2$^+$, EdU$^+$, and Ki67$^+$ T cells from muscle and spleen were cytofluourometrically quantified. As expected, IL-33 increased Treg cell representation, in particular cells

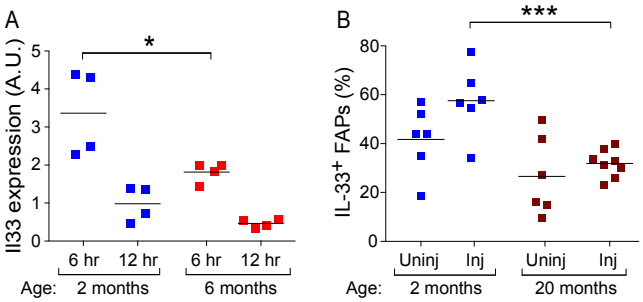

Figure 6. Reduced IL-33 Expression in Skeletal Muscle of Aged Mice

Mice of the designated ages were injected with CTX and expression of IL-33 in tibialis anterior muscle was examined 6–12 hr later.

(A) PCR titration of *Il33* transcripts (fold change versus uninjured). Induction vis-à-vis uninjured muscle is plotted. n = 4 mice from two experiments.

(B) Cytofluorometric analysis of FAPs 12 hr after injury. Gating was performed as in Figure 4D. Summary data from 6–7 mice from two experiments.

The 2-month values correspond to those of Figure 4E. Statistics for this figure as per Figure 1.

displaying ST2 (Figure S5B). According to both EdU incorporation and Ki67 staining, IL-33 induced Treg cell proliferation in both the muscle and spleen (Figures S5C and S5D). In contrast, Tconv cells did not proliferate or accumulate in either the muscle or spleen (Figures S5E–S5G). Similar results (i.e., increased EdU incorporation) came from analogous experiments on young mice (not shown). The Treg cells within muscle that were expanded by IL-33 treatment were typical "muscle Treg cells" according to microarray analysis 4 days after CTX-induced injury (plus IL-33 treatment) of young mice (Figure S5H). In confirmation of the EdU-incorporation and Klrg1-staining experiments, IL-33 induced several pathways related to cell replication, cycling, or proliferation: "cell cycle mitotic" ($p < 8 \times 10^{-8}$), "G2M checkpoint" ($p < 8 \times 10^{-8}$), "cell cycle" ($p < 2.5 \times 10^{-7}$), and "mitotic spindle" ($p < 1 \times 10^{-5}$), according to Gene-Set Enrichment Analysis.

To assess the impact of IL-33 supplementation on muscle regeneration in old mice, we again used the milder, more homogeneous cryoinjury model. Injection of IL-33 into 22-month-old mice at the time of cryoinjury also expanded muscle Treg cells (Figure 7B). Results from multiple assays indicated a statistically significant impact on muscle regeneration. First, the representation of satellite cells (defined as Beta1$^+$CXCR4$^+$Lin$^-$Sca1$^-$ [Cerletti et al., 2008]) increased in response to IL-33 supplementation (Figure 7C), and they were more effective at forming myogenic colonies in vitro (Figure 7D). Second, whole-muscle transcriptomics showed a strong enrichment for the "muscle homeostasis/function" signature in IL-33-, but not PBS-, treated old mice, and less apparent skewing of the "muscle repair/regeneration" signature (Figure 7E). In addition, IL-33-treated old mice showed a striking enrichment and impoverishment of the signatures that were previously determined (Burzyn et al., 2013) to be up- or downregulated, respectively, in mice injected with Areg (Figure 7F). This muscle Treg cell product is a member of the epidermal growth factor family and enhances regeneration through a direct impact on muscle progenitor cells (Burzyn et al., 2013). Third, histologic analysis illustrated superior muscle regeneration in old mice supplemented with IL-33 (Figure 7G). There was an elevated number of regenerating, centrally nucleated, myofibers; an evident skewing in their size distribution to higher values; and a higher average myofibril cross-sectional area (Figure 7H).

DISCUSSION

Acute injury of skeletal muscle in young mice provokes the local accumulation of a special population of Foxp3$^+$CD4$^+$ Treg cells within days (Burzyn et al., 2013). These cells have a transcriptome and TCR repertoire distinct from those of other Treg cell populations, adapted for optimally surviving and operating in the muscle, and thereby promoting effective repair. We now report that the accumulation of Treg cells in injured skeletal muscle profoundly declines with age, paralleling a degradation of repair and regeneration processes. Our results raise several points that merit further discussion.

First, the reduced accumulation of Treg cells in muscle of old mice reflected defects in multiple aspects of their population dynamics: recruitment, proliferation, and retention. That the muscle Treg cell population was so dependent on speedy recruitment from the circulation makes an interesting contrast with the behavior of its counterpart VAT Treg cell population, which is seeded in the first few weeks of life and is self-contained thereafter, with little detectable migration into or out of it (Kolodin et al., 2015). RNA-seq analysis revealed that circulating (i.e., splenic) Treg cells of young and aged mice differentially expressed genes encoding several chemokine receptors, e.g., CXCR6 and CCR7 (lower in aged mice) and CCR5 and CCR3 (higher in aged mice). Several of these differences have been noted previously (Mo et al., 2003). In addition, the gene encoding the S1P1 receptor was downregulated in splenocytes of old mice. One or more of these differences could underlie the reduced egress of Treg cells from the LNs of aged mice and/or their diminished recruitment to injured muscle. The lower S1P1 expression is a good candidate for the former because signaling through this receptor is known to control egress of most lymphocyte populations from lymphoid organs (Schwab and Cyster, 2007) and S1P1 receptor antagonism at the time of injury blocked Treg cell recruitment to the muscle. Less CCR7 could also promote retention of Treg cells in LNs, as has been reported in another system (Ishimaru et al., 2010). The downregulation of *Itgae* expression in Treg cells in muscle of aged mice could at least partially explain their reduced retention therein because the adhesion molecule it encodes, CD103, has been shown to drive tissue retention of Treg cells (Suffia et al., 2005).

Second, we found IL-33 to be an important regulator of muscle Treg cell homeostasis. Although initial studies had emphasized the role of this cytokine in driving T helper 2 (Th2) cell responses, primarily through an impact on type 2 innate lymphoid cells (ILCs) and anti-inflammatory macrophages (Garlanda et al., 2013; Molofsky et al., 2013), more recent work highlighted its ability to expand Treg cell populations (Turnquist et al., 2011; Matta et al., 2014; Schiering et al., 2014). Results from our loss- and gain-of-function experiments indicated a substantially more potent effect of IL-33 on muscle Treg cells than on lymphoid-tissue Treg cells, parallel to what we previously documented for VAT Treg cells (Kolodin et al., 2015). This difference in potency is also reflected in expression of the IL-33 receptor,

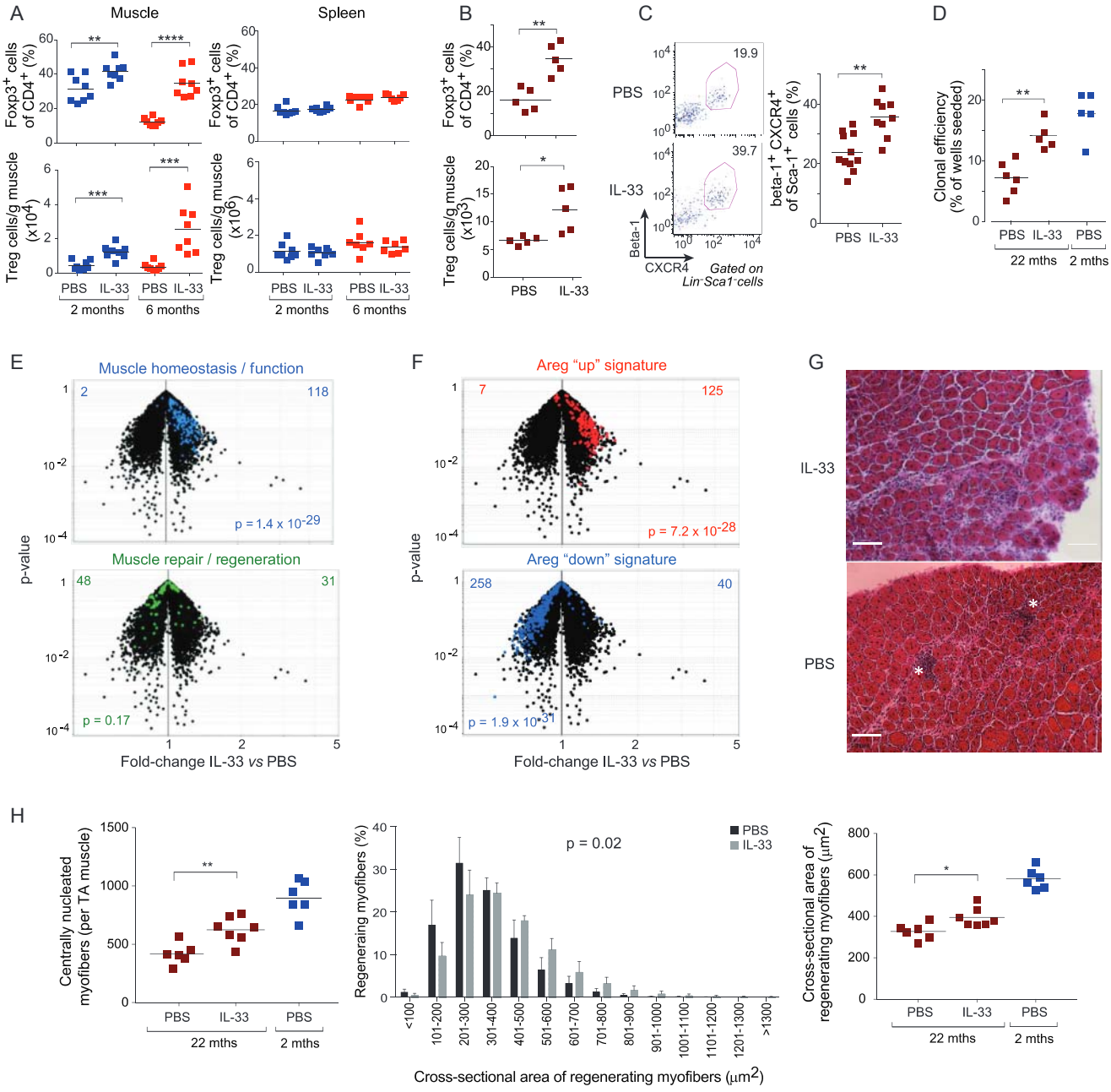

Figure 7. Restoration of the Treg Cell Population in Injured Muscle of Old Mice through IL-33 Supplementation, Promoting Regeneration

(A) Expansion of Treg cell populations in IL-33-treated mice. 2-month-old versus 6-month-old mice were i.m. injected with 0.3 mg/muscle rIL-33 in PBS or just PBS in addition to CTX, and the indicated tissues were examined cytofluorometrically 6 days later. Summary data for eight mice from two experiments.

(B–H) Improvement in muscle regeneration by IL-33 treatment. 22-month-old mice were ip-injected with rIL-33 (2 mg) or PBS the day prior to and the day after cryoinjury and were examined 4 days later. 2-month-old regeneration controls (Burzyn et al., 2013) were not IL-33 treated.

(B) Muscle Treg cell population expansion. Summary data for n = 5 mice from two experiments.

(C) Augmentation of muscle satellite cells in IL-33-treated injured mice. Representative dot plots (left) and summary data (right). Numbers refer to the fraction of $Lin^{-}Sca1^{-}$ cells. n = 9–11 mice from three experiments.

(D) Improved clonal efficiency in IL-33-treated injured mice. Muscle satellite cells were sequentially double-sorted according to the (C) gates, plating individual cells into single wells. Clones were scored after 7 days of culture. Each dot represents a single mouse. Data from three experiments.

(E and F) Microarray assessment of muscle regeneration. Whole-muscle RNA was isolated from 22-month-old mice 8 days after cryoinjury, and the differential expression of diagnostic transcript signatures in the presence and absence of IL-33 treatment were depicted on volcano plots.

(E) The validated regeneration signatures described in the legend to Figure 3E.

(F) The sets of genes previously determined (Burzyn et al., 2013) to be induced (red) or repressed (blue) upon recombinant Areg injection, which was documented to improve muscle regeneration. Values at the top refer to the numbers of genes over- (right) or under- (left) represented after IL-33 (versus PBS) injection.

(legend continued on next page)

ST2: Treg cells in muscle and adipose tissue display substantially more than do their lymphoid-tissue counterparts. Thus, IL-33 might be most relevant for homeostasis of parenchymal tissue Treg cell populations, probably a manifestation of this cytokine's alarmin function, evident in the rapid spike of IL-33 expression in skeletal muscle in response to injury. The IL-33 effect in muscle seemed to be primarily a local one because the representation of Treg cells in Treg-*Il1rl1*mut mice was normal the day after injury—they just failed to accumulate thereafter—and because IL-33 supplementation did not enhance recruitment of circulating Treg cells to the muscle.

Third, the identity of the major IL-33-producing cell type in skeletal muscle was not anticipated. The phenotype of these cells is reminiscent of that of LN fibroblastic reticular cells (FRCs)—$CD45^{-}CD31^{-}PDGFRa^{+}PDPN(Gp38)^{+}$—which have indeed been reported to express abundant *Il33* transcripts (Malhotra et al., 2012). Muscle IL-33 expressers also displayed a constellation of cell-surface markers typical of FAPs: $CD45^{-}CD31^{-}Sca1^{+}PDGFRa^{+}$. FAPs, which can engender both fibroblasts and adipocytes, have been attributed a substantial role in the regeneration of myofibers and in fat deposition within aged skeletal muscle (Joe et al., 2010; Uezumi et al., 2010). It was recently suggested that eosinophil-produced IL-4 and/or IL-13 signals serve as a switch between the two FAP fates, promoting their proliferation to support myogenesis while inhibiting their differentiation into adipocytes (Heredia et al., 2013). FAP-produced IL-33 should be able to sustain $ST2^{+}$ type-2 ILCs in muscle in addition to Treg cells, which would have the potential to feedback positively on eosinophils and anti-inflammatory macrophages via ILC-produced IL-5 and IL-13, as has been reported in VAT (Molofsky et al., 2013). Thus, there is likely to be a complex interplay between innate and adaptive immunocytes, supporting stromal cells, and myocytes in regenerating muscle, as was recently argued for adipose tissue (Molofsky et al., 2015). Nonetheless, the diminished Treg cell accumulation in injured muscle of Treg-*Il1rl1*mut mice argues for a direct link between FAPs and Treg cells via IL-33, as does the fact that IL-33 can induce proliferation of and transcriptional changes within isolated Treg cells in culture (Vasanthakumar et al., 2015; Schiering et al., 2014).

Lastly, the association between a fraction of the IL-33-producing cells and neural structures within skeletal muscle was quite striking. Muscle spindles, which were parenthesized by IL-33-producing cells, are stretch-sensitive mechanoreceptors, and thereby proprioreceptors, that lie parallel to myofibers and transmit signals back and forth to the spinal cord (Maier, 1997). They host both sensory and motor neurons. Most recently, muscle-spindle feedback was shown to play an essential role in facilitating neural circuit reorganization and directing locomotor recovery after spinal-cord injury (Takeoka et al., 2014). Our finding, together with reports that the IL-33:ST2 axis has a mechanically activated cardioprotective role reflective of heart fibroblast:myocyte cross-talk (Sanada et al., 2007), raises the possibility that IL-33 might operate generally as a mechano-sensitive signal. Indeed, application of mechanical stress to fibroblasts in vitro or in vivo induced IL-33 secretion in the absence of cell necrosis (Kakkar et al., 2012). It might also be worth noting that as many as 1/3 of dispersed brain cells, especially oligodendrocytes and gray-matter astrocytes, were reported to express IL-33, which is released from injured central nervous system (CNS) tissue and promotes recovery after CNS injury (Gadani et al., 2015). Thus, IL-33 is well placed to relay homeostatic signals between the nervous and immune systems in the muscle context.

Age-related sarcopenia and associated defects in muscle repair subsequent to injury or atrophy represent a major health problem with our aging population structure, exerting a strong impact on mobility, independence, and quality of life. The IL-33:ST2 axis seems to be a promising avenue to explore in attempts to address this important problem.

EXPERIMENTAL PROCEDURES

Mice

Most B6 mice were purchased from the Jackson Laboratory. Foxp3-IRES-GFP (Bettelli et al., 2006), Kaede/B6 (Tomura et al., 2008), *Foxp3-cre*YFP (Rubtsov et al., 2008), and *Il1rl1*-flox (Chen et al., 2015) mice were obtained from V. Kuchroo, O. Kanagawa, A. Rudensky, and R. Lee, respectively. Mice lacking ST2 specifically on Treg cells (Treg-*Il1rl1*mut) were generated by crossing the ST2-flox and Foxp3-creYFP lines. B6 mice R 20 months of age (and control 2-month-old mice) were obtained from the National Institute of Aging colony at Charles River Laboratories. All mice were housed in our specific-pathogen-free facilities at Harvard Medical School. Experiments were conducted under protocols approved by Harvard Medical School's Institutional Animal Care and Use Committee. Male mice of the specified ages were used.

Muscle Injury

Routinely, mice were anesthetized with avertin (0.4 mg/g body weight) and injected with 0.03 ml/muscle of *Naja mossambica* cardiotoxin (0.03 mg/ml, Calbiochem or Sigma) in one or more hindlimb muscles. For regeneration studies, TA muscles were exposed to a liquid-nitrogen-chilled metal probe for 8 s.

Transcript Analyses

RNA-seq on ultra-low cell numbers (1–5 3 10^3) and PCR analyses were performed, and the resulting data were analyzed as detailed in the Supplemental Experimental Procedures.

For microarray analysis of whole muscle, the tissue was flash-frozen in liquid nitrogen and homogenized in TRIzol (Invitrogen) before RNA extraction (Painter et al., 2011). Microarray analysis of T cell populations was always done on double-sorted cells. All samples were generated in duplicate or (usually) triplicate. Sample processing and data analysis were performed as previously described (Cipolletta et al., 2012). The "muscle homeostasis/function" and "muscle repair/regeneration" signatures were developed and validated in Burzyn et al. (2013), as were the Areg "up" and "down" signatures.

Assessment of Population Dynamics

To block exit of lymphocytes from peripheral lymphoid organs, mice were treated with an S1P1 receptor agonist. 25 mg/kg FTY720 (Cayman Chemical)

(G) Histologic presentation. Representative H&E-stained sections of tibialis anterior muscle. Representative of two experiments. Asterisks designate immunocyte infiltration. Original magnification is 1003 .

(H) Number (left) and cross-sectional area represented either as the frequency distribution (middle) or mean area (right) of regenerating myofibers per mouse from day 8 cryoinjured TA muscle. Summary data for 6–7 mice from two experiments. 2-month-old regeneration controls, the same as Figure 3G, were not IL-33 treated. Statistics as per Figure 1, except p values for (E) and (F) come from the chi-square test and for the middle plot of (H) from the t test of weighted sum. See also Figures S4 and S5.

was i.p. injected prior to injury and daily thereafter. The Kaede Tg mouse system was used to monitor cell migration from the CLNs to hindlimb muscles, draining LNs (ILNs), and non-draining LNs (ALNs); or from TA muscle to the ILNs and ALNs. Details are presented in the Supplemental Experimental Procedures. For quantification of T cell proliferation in vivo, 1 mg EdU was i.p. injected, and 12 or 24 hr later, cells were processed for detection by the Click-iT EdU kit according to the manufacturer's protocol (Molecular Probes).

Clonal Myogenesis Assay

Satellite cells (CD45$^-$Sca-1$^-$CD11b$^-$CXCR4$^+$b1-integrin$^+$) were first sorted in bulk and then individually into 96-well plates coated with collagen (1 mg/ml, Sigma) and laminin (10 mg/ml, Invitrogen). Cells were cultured in F10 medium with 20% horse serum and 5 ng/ml bFGF (Sigma) for 7 days, with fresh bFGF added daily. Wells containing myogenic colonies were scored by brightfield microscopy on day 7.

IL-33 Treatments

Recombinant mouse IL-33 (Biolegend) was administered via intramuscular (i.m.) (0.3 mg/muscle) or i.p. (2 mg) injection. Mice treated with IL-33 i.m. received it only at the time of injury; i.p.-treated mice were given IL-33 the day prior to and the day after injury.

ACCESSION NUMBERS

Microarray/RNA-seq data are available from the National Center for Biotechnology Information/Gene Expression Omnibus repository under accession numbers GEO: GSE76722, GSE76733, GSE76695, and GSE76697.

SUPPLEMENTAL INFORMATION

Supplemental Information includes five figures, one table, and Supplemental Experimental Procedures (including isolation and characterization of muscle leukocytes, myofiber-associated cells, and fibro/adipocyte progenitors and histological analyses) and can be found with this article online at http://dx.doi.org/10.1016/j.immuni.2016.01.009.

AUTHOR CONTRIBUTIONS

Conceptualization, W.K., D.B., M.P., K.K.W., A.J.W., and D.M.; Investigation, W.K., D.B., M.P., and K.K.W.; Resources, Y.C.J.; Writing – Original Draft, W.K. and D.M.; Writing – Review & Editing, W.K., D.B., M.P., K.K.W., Y.C.J., A.J.W., C.B., and D.M.; Supervision, A.J.W. and D.M.; Project Administration, A.J.W., C.B., and D.M.; Funding Acquisition, A.J.W. and D.M.

ACKNOWLEDGMENTS

We thank N. Asinovski, R. Cruse, K. Hattori, D. Jepson, A. Ortiz-Lopez, H. Paik, A. Rhoads, G. Buruzula, and J. LaVecchio for technical support; R. Lee for the ST2-flox mice; E. Estrella, and L. Kunkel for the human samples and for technical advice; and Drs. I. Chiu, A. Magnuson, J. Sanes, and B. Spiegelman for helpful discussions. This work was funded by the JPB Foundation and by NIH grants R01DK092541 to D.M. and R01AG033053 and U01HL100402 to A.J.W., who was also an Early Career Scientist at the Howard Hughes Institute. W.K. was supported by fellowships from the NIH (T32-GM007753 and F30AG046045). Cell sorting was performed under NIH P30DK036836.

Received: June 30, 2015
Revised: October 14, 2015
Accepted: November 17, 2015
Published: February 9, 2016

REFERENCES

Arnold, L., Henry, A., Poron, F., Baba-Amer, Y., van Rooijen, N., Plonquet, A., Gherardi, R.K., and Chazaud, B. (2007). Inflammatory monocytes recruited after skeletal muscle injury switch into antiinflammatory macrophages to support myogenesis. J. Exp. Med. *204*, 1057–1069.

Bettelli, E., Carrier, Y., Gao, W., Korn, T., Strom, T.B., Oukka, M., Weiner, H.L., and Kuchroo, V.K. (2006). Reciprocal developmental pathways for the generation of pathogenic effector TH17 and regulatory T cells. Nature *441*, 235–238.

Brack, A.S., Conboy, M.J., Roy, S., Lee, M., Kuo, C.J., Keller, C., and Rando, T.A. (2007). Increased Wnt signaling during aging alters muscle stem cell fate and increases fibrosis. Science *317*, 807–810.

Burzyn, D., Kuswanto, W., Kolodin, D., Shadrach, J.L., Cerletti, M., Jang, Y., Sefik, E., Tan, T.G., Wagers, A.J., Benoist, C., and Mathis, D. (2013). A special population of regulatory T cells potentiates muscle repair. Cell *155*, 1282–1295.

Cayrol, C., and Girard, J.P. (2014). IL-33: an alarmin cytokine with crucial roles in innate immunity, inflammation and allergy. Curr. Opin. Immunol. *31*, 31–37.

Cerletti, M., Jurga, S., Witczak, C.A., Hirshman, M.F., Shadrach, J.L., Goodyear, L.J., and Wagers, A.J. (2008). Highly efficient, functional engraftment of skeletal muscle stem cells in dystrophic muscles. Cell *134*, 37–47.

Chen, W.Y., Hong, J., Gannon, J., Kakkar, R., and Lee, R.T. (2015). Myocardial pressure overload induces systemic inflammation through endothelial cell IL-33. Proc. Natl. Acad. Sci. USA *112*, 7249–7254.

Cipolletta, D., Feuerer, M., Li, A., Kamei, N., Lee, J., Shoelson, S.E., Benoist, C., and Mathis, D. (2012). PPAR-g is a major driver of the accumulation and phenotype of adipose tissue Treg cells. Nature *486*, 549–553.

Conboy, I.M., Conboy, M.J., Wagers, A.J., Girma, E.R., Weissman, I.L., and Rando, T.A. (2005). Rejuvenation of aged progenitor cells by exposure to a young systemic environment. Nature *433*, 760–764.

Feuerer, M., Herrero, L., Cipolletta, D., Naaz, A., Wong, J., Nayer, A., Lee, J., Goldfine, A.B., Benoist, C., Shoelson, S., and Mathis, D. (2009). Lean, but not obese, fat is enriched for a unique population of regulatory T cells that affect metabolic parameters. Nat. Med. *15*, 930–939.

Gadani, S.P., Walsh, J.T., Smirnov, I., Zheng, J., and Kipnis, J. (2015). The glia-derived alarmin IL-33 orchestrates the immune response and promotes recovery following CNS injury. Neuron *85*, 703–709.

Garlanda, C., Dinarello, C.A., and Mantovani, A. (2013). The interleukin-1 family: back to the future. Immunity *39*, 1003–1018.

Heredia, J.E., Mukundan, L., Chen, F.M., Mueller, A.A., Deo, R.C., Locksley, R.M., Rando, T.A., and Chawla, A. (2013). Type 2 innate signals stimulate fibro/adipogenic progenitors to facilitate muscle regeneration. Cell *153*, 376–388.

Ishimaru, N., Nitta, T., Arakaki, R., Yamada, A., Lipp, M., Takahama, Y., and Hayashi, Y. (2010). In situ patrolling of regulatory T cells is essential for protecting autoimmune exocrinopathy. PLoS ONE *5*, e8588.

Jang, Y.C., Sinha, M., Cerletti, M., Dall'Osso, C., and Wagers, A.J. (2011). Skeletal muscle stem cells: effects of aging and metabolism on muscle regenerative function. Cold Spring Harb. Symp. Quant. Biol. *76*, 101–111.

Joe, A.W., Yi, L., Natarajan, A., Le Grand, F., So, L., Wang, J., Rudnicki, M.A., and Rossi, F.M. (2010). Muscle injury activates resident fibro/adipogenic progenitors that facilitate myogenesis. Nat. Cell Biol. *12*, 153–163.

Kakkar, R., Hei, H., Dobner, S., and Lee, R.T. (2012). Interleukin 33 as a mechanically responsive cytokine secreted by living cells. J. Biol. Chem. *287*, 6941–6948.

Kolodin, D., van Panhuys, N., Li, C., Magnuson, A.M., Cipolletta, D., Miller, C.M., Wagers, A., Germain, R.N., Benoist, C., and Mathis, D. (2015). Antigen- and cytokine-driven accumulation of regulatory T cells in visceral adipose tissue of lean mice. Cell Metab. *21*, 543–557.

Kunkel, G.T., Maceyka, M., Milstien, S., and Spiegel, S. (2013). Targeting the sphingosine-1-phosphate axis in cancer, inflammation and beyond. Nat. Rev. Drug Discov. *12*, 688–702.

Maier, A. (1997). Development and regeneration of muscle spindles in mammals and birds. Int. J. Dev. Biol. *41*, 1–17.

Malhotra, D., Fletcher, A.L., Astarita, J., Lukacs-Kornek, V., Tayalia, P., Gonzalez, S.F., Elpek, K.G., Chang, S.K., Knoblich, K., Hemler, M.E., et al.; Immunological Genome Project Consortium (2012). Transcriptional profiling of stroma from inflamed and resting lymph nodes defines immunological hallmarks. Nat. Immunol. *13*, 499–510.

Matta, B.M., Lott, J.M., Mathews, L.R., Liu, Q., Rosborough, B.R., Blazar, B.R., and Turnquist, H.R. (2014). IL-33 is an unconventional Alarmin that stimulates IL-2 secretion by dendritic cells to selectively expand IL-33R/ST2+ regulatory T cells. J. Immunol. *193*, 4010–4020.

Mo, R., Chen, J., Han, Y., Bueno-Cannizares, C., Misek, D.E., Lescure, P.A., Hanash, S., and Yung, R.L. (2003). T cell chemokine receptor expression in aging. J. Immunol. *170*, 895–904.

Molofsky, A.B., Nussbaum, J.C., Liang, H.E., Van Dyken, S.J., Cheng, L.E., Mohapatra, A., Chawla, A., and Locksley, R.M. (2013). Innate lymphoid type 2 cells sustain visceral adipose tissue eosinophils and alternatively activated macrophages. J. Exp. Med. *210*, 535–549.

Molofsky, A.B., Van Gool, F., Liang, H.E., Van Dyken, S.J., Nussbaum, J.C., Lee, J., Bluestone, J.A., and Locksley, R.M. (2015). Interleukin-33 and interferon-gamma counter-regulate group 2 innate lymphoid cell activation during immune perturbation. Immunity *43*, 161–174.

Murphy, M.M., Lawson, J.A., Mathew, S.J., Hutcheson, D.A., and Kardon, G. (2011). Satellite cells, connective tissue fibroblasts and their interactions are crucial for muscle regeneration. Development *138*, 3625–3637.

Nikolich-Žugich, J. (2014). Aging of the T cell compartment in mice and humans: from no naive expectations to foggy memories. J. Immunol. *193*, 2622–2629.

Painter, M.W., Davis, S., Hardy, R.R., Mathis, D., and Benoist, C.; Immunological Genome Project Consortium (2011). Transcriptomes of the B and T lineages compared by multiplatform microarray profiling. J. Immunol. *186*, 3047–3057.

Rubtsov, Y.P., Rasmussen, J.P., Chi, E.Y., Fontenot, J., Castelli, L., Ye, X., Treuting, P., Siewe, L., Roers, A., Henderson, W.R., Jr., et al. (2008). Regulatory T cell-derived interleukin-10 limits inflammation at environmental interfaces. Immunity *28*, 546–558.

Sanada, S., Hakuno, D., Higgins, L.J., Schreiter, E.R., McKenzie, A.N., and Lee, R.T. (2007). IL-33 and ST2 comprise a critical biomechanically induced and cardioprotective signaling system. J. Clin. Invest. *117*, 1538–1549.

Schiering, C., Krausgruber, T., Chomka, A., Fröhlich, A., Adelmann, K., Wohlfert, E.A., Pott, J., Griseri, T., Bollrath, J., Hegazy, A.N., et al. (2014). The alarmin IL-33 promotes regulatory T-cell function in the intestine. Nature *513*, 564–568.

Schwab, S.R., and Cyster, J.G. (2007). Finding a way out: lymphocyte egress from lymphoid organs. Nat. Immunol. *8*, 1295–1301.

Sinha, M., Jang, Y.C., Oh, J., Khong, D., Wu, E.Y., Manohar, R., Miller, C., Regalado, S.G., Loffredo, F.S., Pancoast, J.R., et al. (2014). Restoring systemic GDF11 levels reverses age-related dysfunction in mouse skeletal muscle. Science *344*, 649–652.

Suffia, I., Reckling, S.K., Salay, G., and Belkaid, Y. (2005). A role for CD103 in the retention of CD4+CD25+ Treg and control of *Leishmania major* infection. J. Immunol. *174*, 5444–5455.

Takeoka, A., Vollenweider, I., Courtine, G., and Arber, S. (2014). Muscle spindle feedback directs locomotor recovery and circuit reorganization after spinal cord injury. Cell *159*, 1626–1639.

Tidball, J.G., and Villalta, S.A. (2010). Regulatory interactions between muscle and the immune system during muscle regeneration. Am. J. Physiol. Regul. Integr. Comp. Physiol. *298*, R1173–R1187.

Tomura, M., Yoshida, N., Tanaka, J., Karasawa, S., Miwa, Y., Miyawaki, A., and Kanagawa, O. (2008). Monitoring cellular movement in vivo with photoconvertible fluorescence protein "Kaede" transgenic mice. Proc. Natl. Acad. Sci. USA *105*, 10871–10876.

Turnquist, H.R., Zhao, Z., Rosborough, B.R., Liu, Q., Castellaneta, A., Isse, K., Wang, Z., Lang, M., Stolz, D.B., Zheng, X.X., et al. (2011). IL-33 expands suppressive CD11b+ Gr-1(int) and regulatory T cells, including ST2L+ Foxp3+ cells, and mediates regulatory T cell-dependent promotion of cardiac allograft survival. J. Immunol. *187*, 4598–4610.

Uezumi, A., Fukada, S., Yamamoto, N., Takeda, S., and Tsuchida, K. (2010). Mesenchymal progenitors distinct from satellite cells contribute to ectopic fat cell formation in skeletal muscle. Nat. Cell Biol. *12*, 143–152.

Vasanthakumar, A., Moro, K., Xin, A., Liao, Y., Gloury, R., Kawamoto, S., Fagarasan, S., Mielke, L.A., Afshar-Sterle, S., Masters, S.L., et al. (2015). The transcriptional regulators IRF4, BATF and IL-33 orchestrate development and maintenance of adipose tissue-resident regulatory T cells. Nat. Immunol. *16*, 276–285.

Villalta, S.A., Rosenthal, W., Martinez, L., Kaur, A., Sparwasser, T., Tidball, J.G., Margeta, M., Spencer, M.J., and Bluestone, J.A. (2014). Regulatory T cells suppress muscle inflammation and injury in muscular dystrophy. Sci. Transl. Med. *6*, 258ra142.